

혈관 유연성을 고려한 경동맥 분기부 모델 혈류역학 해석

웬민투안* · 이상욱[†]

Numerical Study on Blood Flow Dynamics and Wall Mechanics in a Compliant Carotid Bifurcation Model

Minh Tuan Nguyen and Sang-Wook Lee

Abstract. Blood flow simulations in an realistic carotid bifurcation model with considering wall compliance were carried out to investigate the effect of wall elasticity on the wall shear stress and wall solid stress. Canonical waveforms of flow rates and pressure in carotid arteries were imposed for boundary conditions. Compared to a rigid wall model, we found an increased recirculation region at the carotid bulb and an overall reduction of wall shear stress in a compliant model. Additionally, there was appreciable change of flow rate and pressure wave in longitudinal direction. Both solid and wall shear stress concentration occur at the bifurcation apex.

Key Words : Fluid-Structure Interaction(유체-구조 상호작용), Carotid Bifurcation(경동맥 분기부), 혈류유동(Blood Flow), 혈관벽 유연성(Vessel Wall Compliance)

1. Introduction

Atherosclerosis is a chronic cardiovascular disease developing over decades and the leading cause of myocardial infarction, stroke and other vascular diseases. It leads to significant narrowing or occluding of blood vessel lumen. Many studies exhibited that the initiation and development of atherosclerosis is affected by local biomechanical stimuli. In a investigation on carotid arteries wall dynamics, mechanical stress concentration at the bifurcation was found 9 to 14 times higher to proximal circumferential wall stress and 3 to 4 times larger at sinus bulb⁽¹⁾. Additionally, in a study of Glagov et al.⁽²⁾, it was also revealed that atherosclerotic plaques were built up often at the high concentrating tension area. The study demonstrated the importance of the site of high mechanical stress on initiation and development

of atherosclerotic lesion. In another study⁽³⁾ for investigation of correlation between wall shear stress (WSS) and mechanical stress, the regions of low WSS and high mechanical stress simultaneously have been proposed to associate with atherosclerotic plaque development.

In a continuing attempt to elucidate the role of biomechanical loads on vascular diseases, numerous experimental and computational studies have been carried out using physiologically realistic models. Moreover, with great advancement of medical imaging techniques including magnetic resonance (MR) and computerized tomography (CT) imaging, subject-specific image-based CFD study have been increasingly conducted⁽⁴⁻⁶⁾.

Fluid-structure interaction (FSI) between compliant wall and pulsatile blood flow should be studied for

[†] School of Mechanical Engineering, University of Ulsan
E-mail : leesw@ulsan.ac.kr

* Department of Mechanical Engineering, University of Ulsan

further deeply understand the effect of biomechanical forces on biological response of blood vessel. In the FSI simulation, governing equations of blood flow and vessel wall motion are solved simultaneously. In the previous FSI study⁽⁴⁾ with considering compliant wall motion as well as in vivo imaged geometry, it was found that vessel wall compliance creates non-negligible vessel motion. In addition, a comparison of wall stress pattern and behavior of flow field between rigid and compliant wall models has shown that flow separation and recirculation often occurring at the sinus bulb is appreciably reduced in compliant wall model and that oscillating WSS decreases about 25% of the one from the rigid wall.

In the present study, an realistic carotid bifurcation model was used to carry out FSI simulations with aims of investigation to wall compliance effect on biomechanical forces.

2. Methods

2.1 Carotid Bifurcation Model and Boundary Conditions

A realistic three-dimensional carotid bifurcation model was constructed using computer-aided design software (CATIA, Dassault systems, France) based on representative dimensions of in vivo normal healthy carotids (ref. Fig. 1).

For boundary conditions, the canonical pulsatile flow rates derived from in vivo measurement data by phase-contrast MR were specified at the common carotid artery (CCA) and the external carotid artery (ECA)⁽⁷⁻⁸⁾. A corresponding time-varying pressure condition based on Perktold et al.⁽⁴⁾ was imposed at the internal carotid artery (ICA).

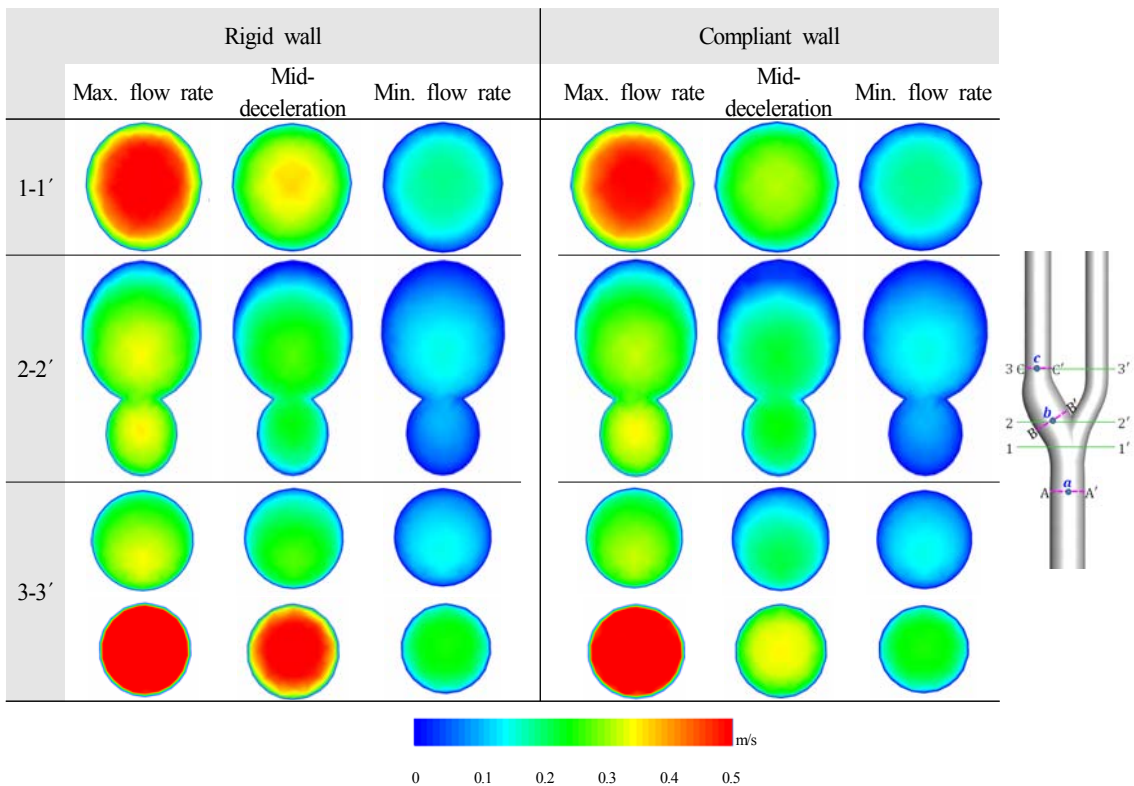


Fig. 1. Comparisons of axial velocity profiles at three different locations and cardiac phases

2.2 Mechanical Properties of the Carotid

The normal wall thickness of carotid artery was reported to be about 8-10% of the arterial diameter in healthy subjects. Since this is relatively small, we modelled the carotid wall as thin-shell structure with a constant wall thickness of $t = 0.6$ mm. In this model, the middle surface is represented as a reference surface and the mechanical behavior of reference surface is computed. The strain is limited to vary only in the radial direction and corresponding stress distribution was computed by numerical integration. The carotid wall was assumed to be an isotropic, linear, elastic with a Young's Modulus of $E = 2.6 \times 10^5$ N/m² and a Poisson's ratio $\nu = 0.45$ for simplification.

2.3 Numerical Methods

A commercial finite element software (ADINA, ADINA R & D, Inc. Watertown, MA) was employed to solve the equation of motion for fluid and solid simultaneously, in a coupled manner.

A fully coupled FSI simulation using an arbitrary Lagrangian-Eulerian formulation was conducted under pulsatile flow condition.

For computational grid, fluid domain was divided into 170,562 tetrahedral elements with 64,001 nodes and the elastic wall composed of 13,414 shell elements after grid convergence test with different set of computational grid sizes. A fine prism mesh was generated near the wall region. The coupled model results in a set of hemodynamic data including velocity, pressure, WSS in fluid domain and mechanical data containing wall displacement and von Mises stress distribution on the arterial wall.

For the purpose of comparison, a non-distensible rigid wall model has also been computed.

3. Results and Discussion

3.1 Axial Velocity distribution, Time-Varying Flow Rates and Pressure Waveform

Axial velocity distributions at three different locations

were compared between rigid and compliant wall simulations in Fig. 1. Although only minor difference can be seen overall, low velocity region at the outer wall of the ICA apparently becomes larger in the compliant wall model in the mid-deceleration phase, with significant reduction of flow rate to the ECA. Comparisons of time-varying flow rates at three different locations of the CCA and the ICA were presented in Fig. 2. It was shown that the pulsatility of flow rate wave becomes larger in the compliant wall model compared to the rigid model. This was most pronounced at the mid-deceleration phase. In addition, it was exhibited that the pulsatility is amplified along with longitudinal direction, particularly within the ICA distal to the bifurcation.

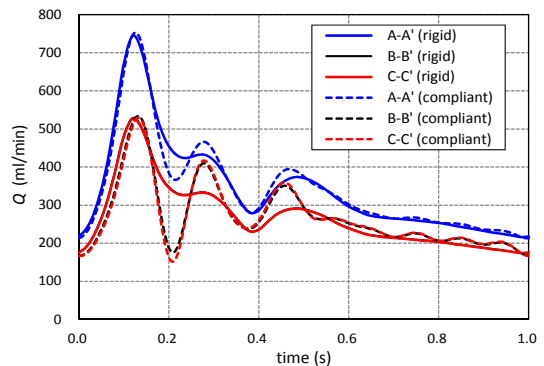


Fig. 2. Comparison of time-varying flow rate waveform at three different positions

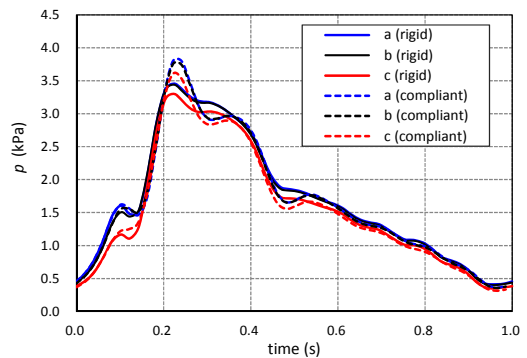


Fig. 3. Comparison of time-varying pressure waveform at three different positions

Fig. 3 presents comparisons of time-varying pressure

profiles at three different positions for the compliant and the rigid wall model. The pressure profile was similar irrespective of wall compliance except at the peak systolic phase in which higher pressure is developed in the compliant model.

3.2 Wall Shear Stress

The WSS, a renowned hemodynamic wall parameters which has long been implicated in correlation with biological response of vascular wall, were presented at the three different cardiac cycle phases including the maximum flow rate, mid-deceleration and minimum flow rate phases (Fig. 4). Although only small reduction of WSS in the compliant model was seen at the peak systolic phase by radial expansion of the vessel wall, considerable difference was observed for the mid-deceleration phase.

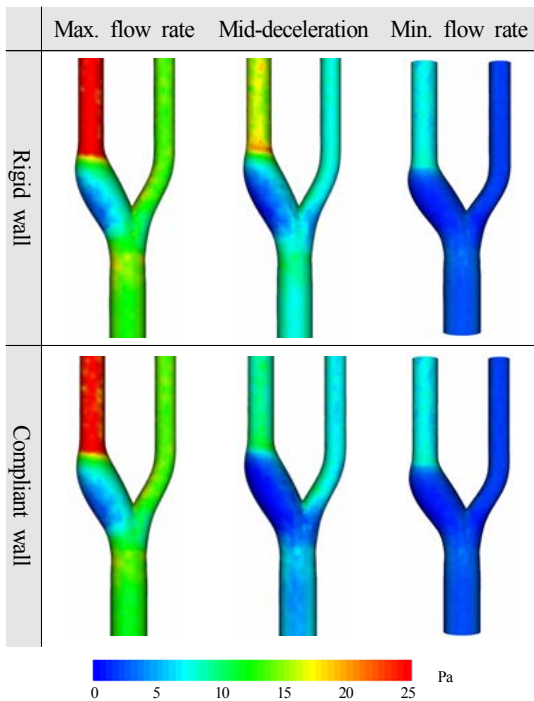


Fig. 4. Comparison of WSS distributions

This may be attributed to the relatively low flow rates at the mid-deceleration phase with increased pulsatility

due to wall compliance as shown in Fig. 2.

3.3 Effective Solid Stress and Wall Displacement

Effective solid stress (von Mises stress) and wall displacement at the corresponding cardiac cycle phases were shown in Figs. 5 and 6, respectively. Relatively higher structural stress was observed around bifurcation region and ICA bulb with the highest value at the bifurcation apex. Maximum wall displacement occurs at the outer wall of the ICA bulb in the mid-decelerating flow rate phase, which is actually a time point when the maximum pressure is loaded. It is worthy of note that rather high structural stress, but relatively low displacement are formed at the outer wall of ECA bifurcation region

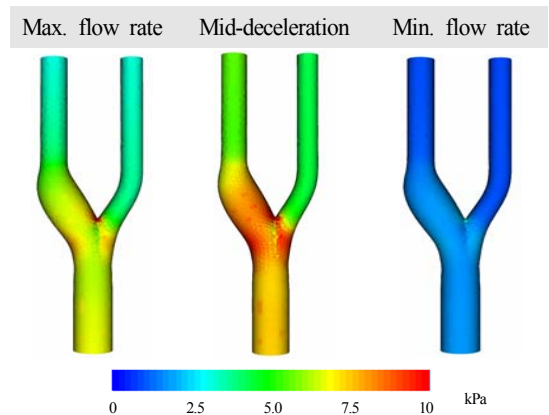


Fig. 5. Von Mises stress distributions

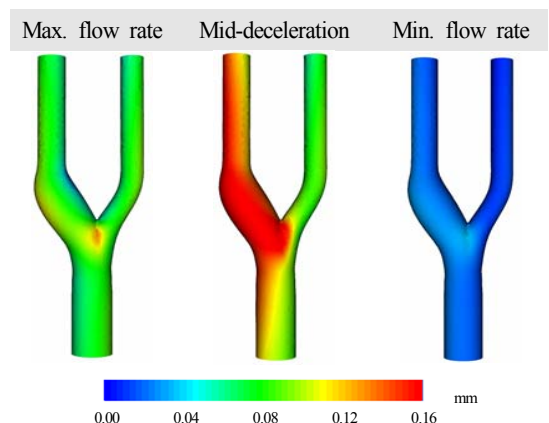


Fig. 6. Wall displacement distributions

4. Conclusion

We conducted FSI simulations for a realistic carotid bifurcation model with linear, elastic wall assumption. It was observed that the recirculation region at the carotid bulb grows and the WSS is reduced on the whole in a compliant model. In addition, there were an appreciable change of the flow rate and pressure waves along longitudinal direction. Apparent concentration of high structural stress and WSS occurs at the bifurcation apex.

REFERENCE

- 1) Salzar, R.S., Thubrikar, M. J. and Eppink, R. T., 1995, "Pressure-induced Mechanical Stress in the Carotid Artery Bifurcation: A Possible Correlation to Atherosclerosis," *J. Biomech.* Vol.28, pp.1333-1340.
- 2) Glagov, S., Rowley D. A. and Kohut R. I., 1961, "Atherosclerosis of Human Aorta and Its Coronary and Renal Arteries. A Consideration of Some Hemodynamic Factors Which May Be Related to the Marked Differences in Atherosclerotic Involvement of the Coronary and Renal Arteries," *Arch. Pathol.* Vol.72, pp.82-95.
- 3) Zhao, S. Z., Ariff, B., Long, Q., Hughes, A. D., Thom, S. A., Stanton, A. V. and Xu, X. Y., 2002, "Inter-individual Variation in Wall Shear Stress and Mechanical Stress Distribution at the Carotid Artery Bifurcation of Healthy Humans," *J. Biomech.* Vol.35, pp.1367-1377
- 4) Perktold, K. and Rappitsch, G., 1995, "Computer Simulation of Local Blood Flow and Vessel Mechanics in a Compliant Carotid Artery Bifurcation Model," *J. Biomech.* Vol.28, pp.845-856.
- 5) Yang, C., Canton, G., Yuan, C., Ferguson, M., Hatsukami, T. S. and Tang, D., "Advanced Human Carotid Plaque Progression Correlates Positively with Flow Shear Stress using Follow-up Scan Data: An in vivo MRI Multi-patient 3D FSI Study," *J. Biomech.* Vol.43, pp.2530-2538.
- 6) Zhao, S. Z., Xu, X. Y., Hughes, A. D., Thom, S. A., Stanton, A. V., Ariff, B. and Long, Q., 2000, "Blood Flow and Vessel Mechanics in a Physiologically Realistic Model of a Human Carotid Arterial Bifurcation," *J. Biomech.*, Vol.33, pp.975 ~ 984.
- 7) Ford, M. D., Alperin, N., Lee, S. H., Holdsworth, D. W. and Steinman, D. A., 2005, "Characterization of Volumetric Flow Rate Waveforms in the Normal Internal Carotid and Vertebral Arteries," *Physiol. Meas.* Vol.26, pp.477-488.
- 8) Marshall, I., Papatheanasopoulou, P. and Wartolowska, K., 2004, "Carotid Flow Rates and Flow Division at the Bifurcation in Healthy Volunteers," *Physiol. Meas.* Vol.25, pp.691-697.